A STATISTICAL COMPARISON OF IMPACT AND AMBIENT TESTING RESULTS FROM THE ALAMOSA CANYON BRIDGE

Scott W. Doebling[1], Charles R. Farrar[2]
Los Alamos National Laboratory
Los Alamos, NM, 87545
Phillip Cornwell[3]
Rose Hulman Institute of Technology,
5500 Wabash Ave.
Terre Haute, IN, 47805

ABSTRACT

In this paper, the modal properties of the Alamosa Canyon Bridge obtained using ambient data are compared to those obtained from impact hammer vibration tests. Using ambient sources of excitation to determine the modal characteristics of large civil engineering structures is desirable for several reasons. The forced vibration testing of such structures generally requires a large amount of specialized equipment and trained personnel making the tests quite expensive. Also, an automated health monitoring system for a large civil structure will most likely use ambient excitation. A modal identification procedure based on a statistical Monte Carlo analysis using the Eigensystem Realization Algorithm is used to compute the modal parameters and their statistics. The results show that for most of the measured modes, the differences between the modal frequencies of the ambient and hammer data sets are statistically significant. However, the differences between the corresponding damping ratio results are not statistically significant. Also, one of the modes identified from the hammer test data was not identifiable from the ambient data set.

INTRODUCTION

Ambient excitation is the most practical type of excitation for testing of large civil engineering structures and for an automated, modal-based health monitoring system designed to assess the deterioration of bridges. Also, an automated health monitoring system for a bridge would undoubtedly use ambient excitation so that the data could be taken periodically and possibly remotely, without taking the bridge out of service. Ambient excitation is widely used as is evident by the large number of papers at the 1996 IMAC conference, over 15, that discuss such testing procedures. However, comparisons of ambient results with those obtained using other more traditional forced vibration methods, especially impact excitation are much rarer [1], [2], and are often done in a laboratory setting. To gain confidence in the data reduction techniques required when using ambient data and in the subsequent results it is desirable, when possible, to compare the results with those obtained using more traditional excitation sources. In this paper the modal properties of the Alamosa Canyon Bridge obtained using ambient data are compared to those obtained from a more traditional impact vibration test.

In a classical impact vibration test, the instrumented structure is impacted with a modal vibration hammer that has a force sensor integrated into its tip. The frequency response function (FRF) between the impact sensor and each response sensor is computed. This procedure is repeated a number of times at a number of different impact locations to get a full characterization of the structure in the frequency band of interest. The modal parameters for the structure are then determined by a curve fit of the measured FRF. Some procedures, such as the Eigensystem Realization Algorithm (ERA) [3], perform the curve fit in the time domain on the inverse discrete Fourier transform of the FRF, known as the discrete impulse response function. This curve fitting theory is based on the assumption that the impulse response function for a multiple degree of freedom system can be represented as the superposition of a number of exponentially decaying sinusoids.

It has been theoretically proven that cross-correlation functions, the inverse Fourier transforms of cross-power spectra (CPS), can also be expressed as summa-

---

1. Technical Staff Member, Engineering Sciences and Applications Division, Engineering Analysis Group (ESA-EA), M/S P946, (505) 667-6950, doebling@lanl.gov.
2. Technical Staff Member, Engineering Sciences and Applications Division, Engineering Analysis Group (ESA-EA)
3. Associate Professor, Dept. of Mechanical Engineering

tions of decaying sinusoids [4]. Each decaying sinusoid has a damped natural frequency and damping ratio that is identical to that of a corresponding structural mode. The primary assumption necessary for this result is that the ambient excitation is essentially white noise. The results are also valid if known harmonic inputs are present. Therefore, correlation functions have the same form as impulse response functions and can also be curve fit using standard modal analysis algorithms such as ERA.

There are two primary drawbacks to performing modal identification on ambient excitation data, however. Because it is not possible to measure the input force when using ambient excitation, the identified mode shapes will not be mass normalized, which is a problem for damage detection techniques that require mass-normalized modes, such as flexibility based damage methods.[5], Also, because the spectra and spatial locations of the input forces cannot be dictated, some vibration modes may not be well excited and therefore may not be identifiable from the data.

When analyzing the results of a modal test, it is important to understand the statistical uncertainty on the results arising from random errors such as electrical noise, slight variations in testing conditions, environmental effects (such and temperature and wind), etc. In this paper, a Monte Carlo analysis procedure is used to compute uncertainty bounds on the identified modal frequencies and damping ratios based on the actual level of measured random noise according to the coherence function. The mean values and the uncertainty bounds for both the modal frequencies and modal damping ratios will be compared for the ambient and hammer impact data sets. The results will demonstrate the relative level of confidence that should be placed in the ambient results as compared to the confidence in the hammer-impact test results.

DESCRIPTION OF THE ALAMOSA CANYON BRIDGE

The Alamosa Canyon Bridge has seven independent spans with a common pier between successive spans. An elevation view of the bridge is shown in Figure 1. The bridge is located on a seldom-used frontage road parallel to Interstate 25 about 10 miles North of the town of Truth or Consequences, New Mexico. Each span consists of a concrete deck supported by six W30x116 steel girders. The roadway in each span is approximately 7.3 m (24 ft) wide and 15.2 (50 ft) long. Integrally attached to the concrete deck is a concrete curb and concrete guard rail. Inspection of the bridge showed that the upper flanges of the beams are imbedded in the concrete. Between adjacent beams are four sets of cross braces equally spaced along the length of the span. The cross braces are channel sections (C12x25). A cross section of the span at a location showing the interior cross braces is shown in Ref. [6]. At the pier the beams rest on rollers, and at the abutment the beams are bolted to a half-roller to approximate a pinned connection.

Figure 1. Elevation View of Alamosa Canyon Bridge

The data acquisition system used in the vibration tests consisted of a Toshiba TECRA 700 laptop computer, four Hewlett Packard (HP) 35652A input modules that provide power to the accelerometers and perform analog to digital conversion of the accelerometer signals, an HP 35651A signal processing module that performs the needed fast Fourier transform calculations, and a commercial data acquisition/signal analysis software package produced by HP. A 3500 watt GENERAC Model R-3500 XL AC generator was used to power this system.

The data acquisition system was set up to measure acceleration and force time histories and to calculate FRFs, power spectral densities (PSDs), cross-power spectra and coherence functions. Sampling parameters were specified that calculated the FRFs from a 16-s time window discretized with 2048 samples. The FRFs were calculated for a frequency range of 0 to 50 Hz at a frequency resolution of 0.0625 Hz. A Force window was applied to the signal from the hammer's force transducer and exponential windows were applied to the signals from the accelerometers. For ambient vibration measurements, Hanning windows were applied to all of the signals. AC coupling was specified to minimize DC offsets.

A PCB model 086B50 impact sledge hammer was used as the impact excitation source. The hammer weighed approximately 53.4 N (12 lbs) and had a 7.6-cm-dia. (3-in-dia) steel head. This hammer has a nominal sensitivity of 0.73 mV/lb and a peak amplitude range of 5000 lbs. A Wilcoxon Research model 736T accelerometer was used to make the driving point acceleration response measurement adjacent to the

hammer impact point. This accelerometer has a nominal sensitivity of 100 mV/g, a specified frequency range of 5 - 15,000 Hz, and a peak amplitude range of 50 g. PCB model 336c integrated circuit piezoelectric accelerometers were used for the vibration measurements. These accelerometers have a nominal sensitivity of 1 V/g, a specified frequency range of 1 - 2000 Hz, and an amplitude range of 4 g. More details regarding the instrumentation can be found in Ref. [6].

A total of 31 acceleration measurements were made on the concrete deck and on the girders below the bridge as shown in Figure 2. Five accelerometers were

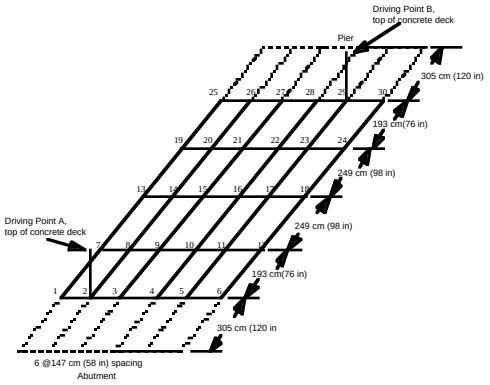

Figure 2. Accelerometer and Impact Locations

spaced along the length of each girder. Because of the limited number of data channels, measurements were not made on the girders at the abutment or at the pier. Two excitations points were located on the top of the concrete deck. Point A was used as the primary excitation location. Point B was used to perform a reciprocity check. The force-input and acceleration-response time histories obtained from each impact were subsequently transformed into the frequency domain so that estimates of the PSDs, FRFs, and coherence functions could be calculated. Thirty averages were typically used for these estimates. With the sampling parameters listed above and the overload reject specified, data acquisition for a specific test usually occurred over a time period of approximately 30 - 45 minutes.

DESCRIPTION OF THE AMBIENT TESTS

All of the results in this paper are from measurements made on span 1 of the bridge, which is located at the far North end. The ambient vibration forces were provided by tractor-trailer trucks descending the hill on the highway next to the bridge, as shown in Figure 3. As the trucks passed onto the Interstate 25 bridge, they induced sufficient ground motions to vibrate the

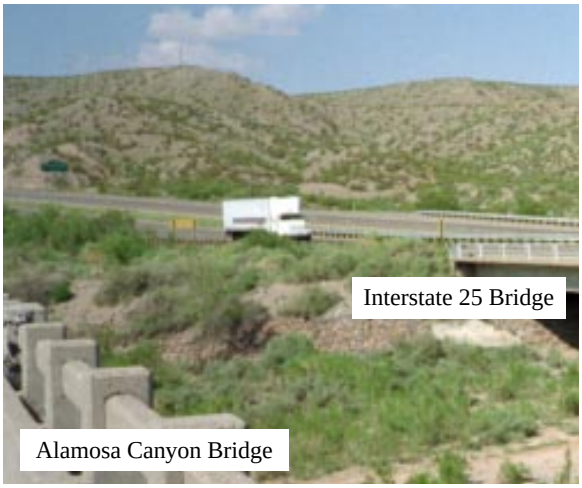

Figure 3. Tractor-Trailer Ambient Excitation Source

Alamosa Canyon Bridge via its piers and abutments. An accelerometer mounted to an aluminum block in the ground midway between the Interstate 25 bridge and the Alamosa Canyon Bridge was used to monitor the level of vibration induced in the ground from the excitation sources. The PSD of the ground motion induced by the trucks (in units of g^2/Hz) is shown in Figure 4. Thirty averages were taken for the ambient

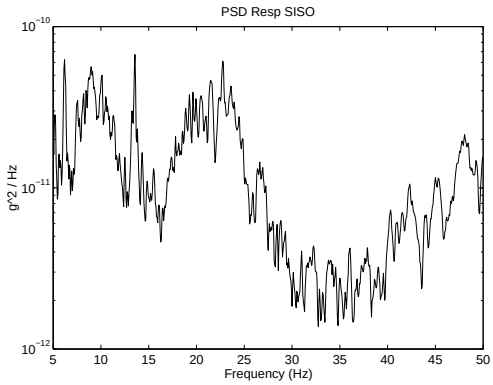

Figure 4. PSD's of Ground Motion Induced by Trucks on Interstate 25 Bridge

tests over a period of approximately 1.5 hours. The accelerometer at location 9 on the sensor diagram of Figure 2 was used as the reference for the CPS computations.

It is known that the dynamic response of this structure exhibits a significant amount of sensitivity to environmental conditions, as shown in Ref. [7]. The ambient excitation data set used in this analysis was taken within 1 hour of the same time of day with approximately the same environmental conditions as the

hammer impact test. Thus it is assumed that the actual dynamic response of the bridge was approximately the same between the impact hammer test and the ambient test. However, it is possible that a slight variability exists between the two data sets.

DISCUSSION OF ANALYSIS TECHNIQUES

The first step in the analysis of the data was the determination of the approximate number of modes to be fit. This number was determined using the Multivariate Mode Indicator Function (MIF) [8] and the Complex Mode Indicator Function (CMIF) [9]. The MIF is an indication of how close to purely imaginary the response is at a particular frequency bin; thus frequencies which correspond to a peak in the MIF can be interpreted as possible modal frequencies. The values are normalized such that the MIF always falls between zero and one. The CMIF is a measure of the maximum singular values of the FRF matrix at each frequency bin. The CMIF also produces a peak at each modal frequency, but these peaks are proportional to the overall magnitude of the frequency response at that bin across all measured degrees of freedom (DOF). This proportionality is advantageous because it allows the user to get a feel for the relative strengths of each mode. However, it has the disadvantage that sometimes particularly strong modes can 'washout' nearby peaks. In this analysis, the CMIF and MIF were computed, and then zoomed to frequency bands of 10 Hz at a time. Approximately 9 modes of significant strength were located between 0 Hz and 30 Hz by inspection of the CMIF and MIF, as shown in Ref. [6].

The next step in the analysis was the application of ERA [3]. The ERA procedure is based upon the formation of a Hankel matrix containing the measured discrete-time impulse response data, computed using the inverse fast Fourier transform of the measured FRFs. The shift in this matrix from one time step to the next is used to estimate a discrete-time state space model for the structure. The current data set contains 31 responses and 1 reference, and a Hankel matrix with 30 block rows and 200 block columns was used.

The model resulting from the ERA analysis had 80 modes, but it was known from examination of the MIF and CMIF that the data contains only about 9 modes in the band of interest. Thus it was necessary to apply some discrimination procedures to select the modes that were physically meaningful. There are three indicators developed specifically for use with ERA [10]: Extended Modal Amplitude Coherence (EMAC), Modal Phase Collinearity (MPC), and Consistent Mode Indicator (CMI), which is the product of EMAC and MPC. EMAC is a measure of how accurately a particular mode projects forward (in time) onto the impulse response data. MPC is a measure of how collinear the phases of the components of a particular complex mode are. If the phases are perfectly linear (i.e. either in phase or 180 degrees out of phase with each other), this mode is exactly proportionately damped, and can then be completely represented by a corresponding real mode shape. Thus, EMAC is a temporal quality measure and MPC is a spatial quality measure. Typically, we start with values of EMAC = 0.7, MPC = 0.7, and CMI = 0.5, and then see if all of the modes of interest (as determined by MIF and CMIF inspection) are preserved. In the current study, all 9 modes of interest passed these criteria, so these values of EMAC, MPC, and CMI were used as the cutoff values.

The next step in the process was the visual inspection of the mode shapes. For a beam or plate-like structure, such as the Alamosa Canyon Bridge, the visual inspection of the mode shapes is particularly useful, because the response shapes are somewhat intuitive. The comparison of the measured modes to the FEM modes was useful as well, and a one-to-one correspondence was found between the 9 measured modes and 9 of the first 10 FEM modes. (One of the first 10 FEM modes was bending in the plane of the deck. This mode was not measured in this test, because all of the sensors were mounted perpendicular to the plane of the deck.)

Statistical uncertainty bounds on the measured frequency response function magnitude and phase were computed from the measured coherence functions, assuming that the errors were distributed in a Gaussian manner, according to the following formulas from Bendat and Piersol [11]:

$$\begin{aligned} \sigma(|H(\omega)|) &= \frac{\sqrt{1-\gamma^2(\omega)}}{|\gamma(\omega)|\sqrt{2n_d}}|H(\omega)| \\ \sigma(\angle H(\omega)) &= \frac{\sqrt{1-\gamma^2(\omega)}}{|\gamma(\omega)|\sqrt{2n_d}}\angle H(\omega) \end{aligned} \tag{1}$$

where $|H(\omega)|$ and $\angle H(\omega)$ are the magnitude and phase angle of the measured FRF, respectively, $\gamma^2(\omega)$ is the coherence function, n_d is the number of measurement averages, and $\sigma(\bullet)$ is the value of 1 standard deviation (68% uncertainty bound). These uncertainty bounds represent a statistical distribution of the FRF based on a realistic level of random noise on the measurement. Once the 1 standard deviation (68% uncertainty) bounds were known, 2 standard deviation (95% uncertainty) bounds were computed. Typical 95% uncertainty bounds on the FRF magnitude and phase for this data set are shown in Figure 5.

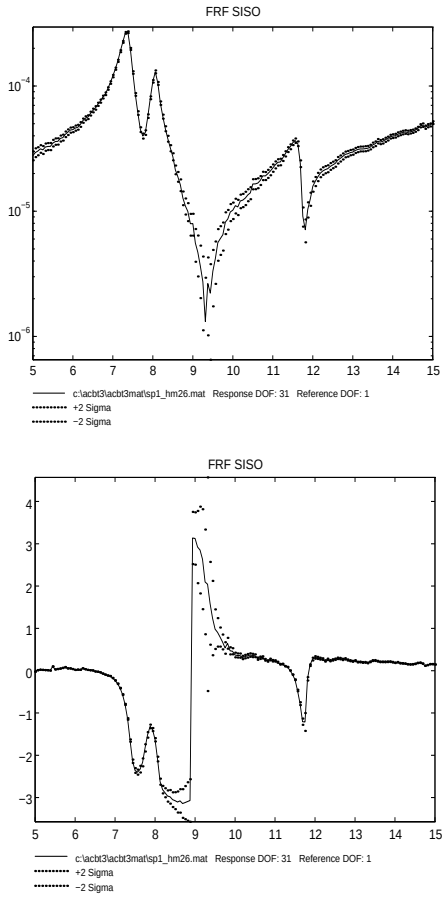

Figure 5. Typical 95% Confidence Bounds on FRF Magnitude and Phase

Monte Carlo Analysis Procedure

Statistical uncertainty bounds on the identified modal parameters (frequencies, damping ratios, and mode shapes) were estimated using the previously determined uncertainty bounds on the FRFs via a Monte Carlo analysis.[12] The basic idea of a Monte Carlo analysis is the repeated simulation of random input data, in this case the FRF with estimated mean and standard deviation values, and compilation of statistics on the output data, in this case the ERA results. For this analysis, the procedure is summarized as:

1. Add Gaussian random noise to the FRFs using the noise standard deviations computed in Eq. (1). This additive noise represents a realistic level of random variations in the measurements.

2. Run the noisy FRF through the ERA identification procedure and apply the modal discrimination using the previously computed parameters.

3. Compute the mean and standard deviation of each modal frequency, damping ratio, and mode shape component over the total number of runs.

4. Repeat steps 1, 2, and 3 until the means and standard deviations calculated in step 3 converge.

For the current study, the convergence took about 100 runs. Tracking the convergence determined the sufficient sample size to provide significant confidence on the statistical estimates. Statistics on the identified modal parameters were computed for both the hammer and ambient data sets using the same identification parameters and modal discrimination criteria.

RESULTS

A comparison of the mean modal frequencies for the 9 identified modes are shown in Table 1. The percent differences between the hammer test and the ambient test range from 0.03% (mode 9) to 3.19% (mode 5), but most are in the vicinity of 1%. It should be noted that mode 7 was not identified in the ambient data set. Presumably, that mode was not sufficiently excited by the ambient excitation forces.

Table 1. Mean Modal Frequency Comparison

Mode	Hammer Data (Hz)	Ambient Data (Hz	% Difference
1	7.376	7.463	1.18%
2	8.042	8.008	-0.42%
3	11.476	11.535	0.51%
4	19.548	19.883	1.72%
5	23.381	22.636	-3.19%
6	25.235	25.557	1.27%
7	25.846	(Missed)	N/A
8	26.885	27.216	1.23%
9	28.128	28.136	0.03%

A comparison of the mean modal damping ratios for the 9 identified modes are shown in Table 2. These values have percent differences ranging from 18% (mode 1) to 109% (mode 5). Overall the errors in the damping ratios are on the order of 50%, with the modes from the hammer impact test typically having the higher damping ratio. It is typically thought that damping levels increase with increasing excitation force level, so that the damping ratios from the hammer data should be higher than the damping ratios

Table 2. Mean Modal Damping Ratio Comparison

Mode	Hammer Data	Ambient Data	% Diff
1	1.54%	1.26%	-18.21%
2	1.19%	0.58%	-51.43%
3	1.13%	0.68%	-40.11%
4	2.17%	1.08%	-50.28%
5	0.96%	2.01%	109.33%
6	2.28%	1.08%	-52.67%
7	0.64%	(Missed)	N/A
8	1.94%	0.93%	-52.21%
9	0.92%	0.75%	-18.92%

from the ambient data. Except for mode 5, this trend is observed.

A comparison of the relative levels of uncertainty between the modal frequencies and damping ratios is shown in Table 3. Columns 2 and 3 are the 95% uncer-

Table 3. Relative 95% Uncertainty Level Comparison

Mode	Hammer Freq 2σ	Ambient Freq 2σ	Hammer Zeta 2σ	Ambient Zeta 2σ
1	0.12%	1.02%	7.81%	51.08%
2	0.13%	0.31%	12.14%	54.43%
3	0.16%	0.12%	12.04%	16.05%
4	0.44%	0.45%	21.95%	50.72%
5	0.61%	1.42%	89.86%	87.91%
6	0.68%	0.66%	23.10%	62.45%
7	0.55%	N/A	109.45%	N/A
8	0.30%	0.15%	18.54%	16.29%
9	0.10%	0.14%	10.41%	19.81%

tainty bounds (2 standard deviations) on the hammer and ambient data modal frequencies, respectively. With the exception of mode 9, the 95% uncertainty bounds on the measured modal frequencies are smaller than the percent differences presented in Table 1. Thus, it can be stated that the frequency differences observed in Table 1 are statistically significant, and are not attributable merely to random disturbances. It is possible that these frequency differences are a result of the fact that these data sets were acquired on different days, albeit under similar environmental conditions.

Columns 4 and 5 in Table 3 are the 95% uncertainty bounds on the identified modal damping ratios. With the exception of modes 3 and 8, the uncertainties on the ambient modal damping ratios are significantly larger than the percent differences between the hammer and ambient modal damping ratios from column 3 of Table 2. Thus, it can be stated for all of the modes (except 3 and 8) that the differences between modal damping ratios observed in Table 2 are most likely the results of random variations in the structural response measurements, and not actual differences in the response of the structure. For modes 3 and 8, the uncertainty levels in the damping ratios are much less than the difference between the hammer and ambient modal damping ratios, indicating that for those two modes, there is a significant difference in the damping response of the structure between the two types of excitation.

CONCLUSIONS

A comparison was made between the statistics on the identified modal frequencies and modal damping ratios of a hammer impact test and an ambient vibration test of the Alamosa Canyon Bridge. The results demonstrate that for most of the measured modes, the differences between the modal frequencies of the ambient and hammer data sets are statistically significant. This difference is potentially attributable to the fact that these data sets were acquired on different days, albeit under similar environmental conditions. However, the differences between the corresponding damping ratio results are not statistically significant. It is therefore not possible to state with significant certainty that the damping ratio is different between the two data sets, even though with the lower excitation level of the ambient test it is expected that the observed damping will be lower. Also, an additional difference between the results is that one of the modes identified from the hammer test data was not identifiable from the ambient data set.

ACKNOWLEDGMENTS

This work was supported by Los Alamos National Laboratory Directed Research and Development Project #95002, under the auspices of the United States Department of Energy. The authors wish to recognize the contributions of Mr. Erik G. Straser and Mr. A. Alex Barron of Stanford University, and Mr. Randall S. Goodman of The University of Colorado at Boulder.

REFERENCES

[1] Kong, F., L. Zhong, and G. Lee, "Responses of a Model Bridge Under Impact and Ambient Excitation", *Proceedings of the 14th International Modal Analysis Conference*, Detroit, MI., 709-716, 1996.

[2] Farrar, C.R., et al., "Dynamic Characterization and Damage Detection in the I-40 Bridge over the Rio Grande," Los Alamos National Laboratory report LA-12767-MS, June, 1994.

[3] Juang, J.N. and Pappa, R.S., "An Eigensystem Realization Algorithm for Modal Parameter Identification and Model Reduction," *Journal of Guidance, Control and Dynamics*, Vol. 8, No. 5, Sept.-Oct. 1985, pp. 620-627.

[4] James III, G.H., T.G. Carne, and J.P. Lauffer, "The Natural Excitation Technique (NExT) for Modal Parameter Extraction from Operating Structures," *The International Journal of Analytical and Experimental Modal Analysis*, Vol. 10, No. 4, 260-277, Oct. 1995.

[5] Toksoy, T. and Aktan, A.E., "Bridge-condition Assessment by Modal Flexibility," *Experimental Mechanics*, Vol. 34, pp. 271–278, 1994.

[6] Doebling, S.W., Farrar, C.R., and Goodman, R.S., "Effects of Measurement Statistics on the Detection of Damage in the Alamosa Canyon Bridge," to appear in *Proc. of the 15th International Modal Analysis Conference*, Orlando, FL, February, 1997.

[7] Farrar, C.R., Doebling, S.W., Cornwell, P.J., and Straser, E.G., "Variability Of Modal Parameters Measured On The Alamosa Canyon Bridge," to appear in *Proc. of the 15th International Modal Analysis Conference*, Orlando, FL, February, 1997.

[8] Allemang, R.J., "Vibrations: Experimental Modal Analysis," University of Cincinnati Class Notes, UC-SDRL-CN-20-263-663/664.

[9] Shih, C.Y., Tsuei, Y.G., Allemang, R.J., Brown, D.L., "Complex Mode Indicator Function and Its Application to Spatial Domain Parameter Estimation," *Mechanical Systems and Signal Processing*, Vol. 2, No. 4, pp. 367-377, 1988.

[10] Pappa, R.S., Elliott, K.B., and Schenk, A., "Consistent-Mode Indicator for the Eigensystem Realization Algorithm," *Journal of Guidance, Control and Dynamics*, Vol. 16, No. 5, Sept.-Oct. 1993, pp. 852–858.

[11] Bendat, J.S. and Piersol, A.G., *Engineering Applications of Correlation and Spectral Analysis*, John Wiley and Sons, New York, 1980, p. 274.

[12] Press, W.H., Teukolsky, S.A., Vetterling, W.T., and Flannery, B.P., *Numerical Recipes in FORTRAN: The Art of Scientific Computing*, Second Edition, Cambridge Univ. Press, 1992, pp. 684-686.